Effect of surface tension on swell-induced surface instability of substrate-confined hydrogel layers†

Min K. Kang and Rui Huang*

Swell-induced surface instability has been observed experimentally in rubbers and gels. Here we present a theoretical model that predicts the critical condition along with a characteristic wavelength for swell-induced surface instability in substrate-confined hydrogel layers. The effect of surface tension is found to be critical in suppressing short-wavelength modes of instability, while the substrate confinement suppresses long-wavelength modes. Together, an intermediate wavelength is selected at a critical swelling ratio for the onset of surface instability. Both the critical swelling ratio and the characteristic wavelength depend on the initial thickness of the hydrogel layer as well as other material properties of the hydrogel. It is found that the hydrogel layer becomes increasingly stable as the initial layer thickness decreases. A critical thickness is predicted, below which the hydrogel layer swells homogeneously and remains stable at the equilibrium state.

1. Introduction

Subjected to mechanical compression, the surface of a rubber block becomes unstable at a critical strain, beyond which sharp folds or creases appear on the surface.[1,2] Similar surface instability has been observed in swelling rubber vulcanizates[3] and polymer gels.[4–7] Such instability may pose a fundamental limit on load-carrying capacity of rubber or on the degree of swelling for gels. On the other hand, the physics of surface instability may be harnessed in the design of responsive "smart" surfaces for novel applications.[8,9] In both cases, theoretical understanding on the critical condition of surface instability as well as subsequent surface pattern evolution is essential.

By considering a half-space of an incompressible neo-Hooken elastic material under mechanical compression, Biot[10] predicted that the surface becomes unstable at a critical level of compression. Later, it was found that Biot's prediction considerably overestimated the critical strain for surface creasing in rubber blocks deformed by bending.[1] A recent paper by Hong *et al.*[11] presented an alternative analysis of surface creasing in rubber based on an energetic consideration and suggested that creasing is a different mode of surface instability in contrast with Biot's periodic surface wave analysis. Several theoretical models have also been proposed for swelling induced surface instability in gels.[4,11–15] At least two questions remain open for gels: (1) What is the critical condition for swelling induced surface instability? (2) What determines the characteristic size of surface patterns formed beyond the critical point?

For the first question, a critical osmotic pressure was suggested based on a composite beam model.[4] Based on their experiments with a hydrogel layer on a rigid substrate, Trujillo *et al.*[6] suggested a critical linear compressive strain of ~33%, or a critical swelling ratio of ~2. Hong *et al.*[11] predicted a critical swelling

ratio of ~2.4. Experimentally, a wide range of critical swelling ratios were observed for different gel systems, from around 2 to 3.7.[3,5,6] In a previous study,[15] we performed a linear perturbation analysis for surface instability of substrate-confined hydrogel layers and predicted a range of critical swelling ratios from about 2.5 to 3.4, depending on the material properties of the hydrogel system. However, two key effects were not considered. First, depending on the kinetics of swelling, the critical swelling ratio for onset of surface instability can potentially be lower due to inhomogeneous transient state of swelling.[16,17] Second, the effect of surface energy or surface tension tends to stabilize the flat surface, which could lead to larger critical swelling ratios, especially for very thin layers.

For the second question, several experimental studies have reported characteristic wavelengths proportional to the initial thickness of the gel.[4,6–8] As discussed in the previous study,[15] while the substrate confinement indeed suppresses long-wavelength modes of surface instability, the confinement effect alone does not lead to a finite characteristic wavelength since the short-wavelength modes are unaffected by the substrate. Two possible mechanisms may be important in addressing this question. For one, the characteristic wavelength may be dynamically determined by the swelling kinetics,[17] similar to wrinkling of an elastic thin film on a viscoelastic substrate.[18–20] Second, the short-wavelength modes of surface instability may be suppressed by surface tension of the hydrogel, which together with the substrate confinement effect would result in a finite wavelength for the surface instability. Alternatively, a strain-gradient effect was suggested to suppress the short-wavelength modes.[12]

The present study focuses on the effects of surface tension on both the critical condition and the characteristic wavelength. Along with a separate study on the effects of swelling kinetics, we aim to establish a vigorous theoretical understanding on swell-induced surface instability of substrate-confined hydrogels. The remainder of this article is organized as follows. Section 2 presents an analytical solution for homogeneous swelling of a hydrogel layer on a rigid substrate, based on a specific material model of neutral polymer hydrogels. A linear perturbation

Department of Aerospace Engineering and Engineering Mechanics, University of Texas at Austin, Austin, TX, 78712. E-mail: ruihuang@mail.utexas.edu; Tel: +1-512-471-7558

analysis is performed in Section 3 to predict onset of surface instability for a homogeneously swollen hydrogel layer. The effect of surface tension is taken into account through the boundary condition. The results are discussed in Section 4. In addition to the critical swelling ratio and the characteristic wavelength, a critical thickness is predicted for thin hydrogel layers, whose surface becomes increasingly stable as the initial layer thickness decreases.

2. Homogeneous swelling of a hydrogel layer

Consider homogeneous swelling of a hydrogel layer attached to a rigid substrate (Fig. 1a), where a Cartesian coordinate system is set up such that $x_2 = 0$ at the hydrogel/substrate interface. At the dry state, the thickness of the hydrogel layer is h_0, while the other two dimensions are assumed to be infinite. Confined by the substrate, the hydrogel layer swells only in the thickness direction with a homogeneous swelling ratio, $\lambda_h = h/h_0 > 1$, where h is the thickness of the swollen hydrogel. The homogeneous swelling ratio can be determined by minimizing the total free energy of the hydrogel system.[15] Using a particular form of the Flory–Huggins free energy function for the hydrogel,[21–23] the homogeneous swelling ratio (λ_h) is obtained as a function of the chemical potential ($\hat{\mu}$) of the external solvent by eqn (2.1):

$$\ln\left(1 - \frac{1}{\lambda_h}\right) + \frac{1}{\lambda_h} + \frac{\chi}{\lambda_h^2} + Nv\left(\lambda_h - \frac{1}{\lambda_h}\right) = \frac{\hat{\mu} - pv}{k_B T} \qquad (2.1)$$

where the material properties of the hydrogel are represented by two dimensionless parameters (Nv and χ). The external chemical

Fig. 1 Schematic illustrations of substrate-confined hydrogel layers. (a) Homogeneous swelling; (b) Onset of swell-induced surface instability; (c) formation of surface creases.

potential in general is a function of the temperature (T) and pressure (p). Assuming an ideal gas phase ($p < p_0$) and an incompressible liquid phase ($p > p_0$) for the solvent, the chemical potential is given by

$$\hat{\mu}(p, T) = \begin{cases} (p - p_0)v, & \text{if } p > p_0; \\ k_B T \ln(p/p_0), & \text{if } p < p_0, \end{cases} \qquad (2.2)$$

where p_0 is the equilibrium vapor pressure of the solvent, v is the volume per solvent molecule, and k_B is the Boltzmann constant.

At a constant temperature (T), eqn (2.1) predicts that the hydrogel layer swells increasingly as the chemical potential increases until it reaches an equilibrium value at the equilibrium vapor pressure of the solvent (i.e., $p = p_0$ and $\hat{\mu} = 0$). In experiments, however, the equilibrium swelling ratio may be reached by immersing the hydrogel in an aqueous solution for a sufficiently long time, while the transient state of swelling may be inhomogeneous. In either case, the equilibrium swelling ratio is a function of temperature, depending on three dimensionless parameters, $\bar{p}_0 = p_0 v/(k_B T)$, Nv, and χ. The first parameter depends on the solvent only. For water at 25 °C, $p_0 \sim 3.2$ kPa, $v \sim 3 \times 10^{-29}$ m³, and thus $\bar{p}_0 \sim 2.3 \times 10^{-5}$, which is relatively small and may be approximately taken to be zero. The second parameter depends on the polymer network of the hydrogel, with N being the effective number of polymer chains per unit volume of the hydrogel at the dry state. The polymer network has an initial shear modulus, $G_0 = Nk_B T$, with typical values from 0.1 kPa to 100 kPa.[6] Thus, the value of Nv ranges from 10^{-6} to 10^{-3}. The third parameter, χ, is a dimensionless quantity characterizing the interaction between the solvent molecules and the polymer, which has been measured and tabulated for many gels.[21] The value of χ also differentiates a good solvent ($\chi < 0.5$) from a poor solvent ($\chi > 0.5$). Taking $\bar{p}_0 = 2.3 \times 10^{-5}$, $Nv = 10^{-3}$, and $\chi = 0.4$, we obtain from eqn (2.1) the equilibrium swelling ratio, $\lambda_h = 5.58$. The equilibrium swelling ratio decreases with increasing values of Nv or χ.

Upon swelling, the confinement by the substrate induces a compressive stress in the hydrogel layer. As in the previous studies,[15,23] the nominal stresses are obtained as a function of the swelling ratio:

$$s_{11} = s_{33} = s_h = -Nk_B T(\lambda_h^2 - 1) - p\lambda_h \qquad (2.3)$$

and $s_{22} = -p$. The true (Cauchy) stresses at the swollen state are related to the nominal stresses as $\sigma_{11} = \sigma_{33} = s_h/\lambda_h = -Nk_B T(\lambda_h - 1/\lambda_h) - p$ and $\sigma_{22} = s_{22} = -p$. Thus, the pressure inside the hydrogel is

$$p_{in} = \frac{1}{3}(\sigma_{11} + \sigma_{22} + \sigma_{33}) = p + \frac{2}{3}Nk_B T\left(\lambda_h - \frac{1}{\lambda_h}\right) \qquad (2.4)$$

It is noted that the internal pressure of the hydrogel is higher than the external pressure (p) of the solvent, analogous to the osmosis phenomenon (i.e., the hydrogel is hypertonic and the external solvent is hypotonic).

As the surface of the hydrogel layer is assumed to remain flat during the homogeneous swelling (Fig. 1a), the presence of a surface tension or surface energy does not have any effect on the one-dimensional (1-D) homogeneous swelling of the hydrogel. We note that this is not the case for un-constrained three-dimensional (3-D) swelling of a hydrogel particle in a solvent, for
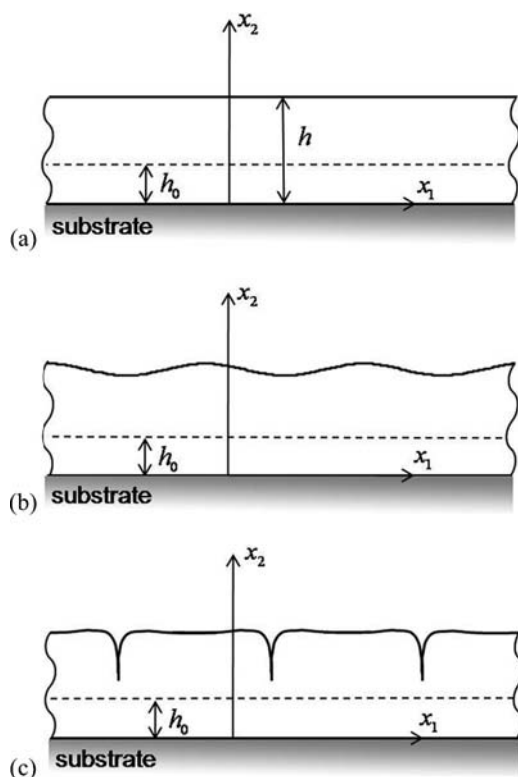
which surface tension does have an effect as the surface area increases during swelling, especially for small-scale hydrogel particles.[24] In the present study, we show that, despite its no-effect on the homogeneous swelling, surface tension plays a critical role in swell-induced surface instability of substrate-confined hydrogel layers.

3. Linear perturbation analysis

Previously we have performed a linear perturbation analysis of the homogeneous solution to predict swell-induced surface instability without considering the effect of surface tension.[15] Following the same procedure, we present here a linear perturbation analysis with the effect of surface tension. As illustrated in Fig. 1, once the surface becomes unstable, it may evolve from a smooth undulation (Fig. 1b) to form localized foldings and surface creases (Fig. 1c).

For a linear stability analysis, a two-dimensional perturbation is assumed with small displacements from the homogeneously swollen state, namely

$$u_1 = u_1(x_1, x_2) \text{ and } u_2 = u_2(x_1, x_2). \quad (3.1)$$

Such a perturbation leads to an inhomogeneous deformation of the hydrogel along with re-distribution of the solvent concentration inside the gel (Fig. 1b). As a result, the stress field becomes inhomogeneous as well. To the leading order of the perturbation, the nominal stresses in the hydrogel are obtained as follows:

$$s_{iJ} \approx Nk_B T[\tilde{F}_{iJ} - (\lambda_h - \xi_h \varepsilon)H_{iJ}] - pH_{iJ} \quad (3.2)$$

where

$$\tilde{F} = \begin{bmatrix} 1 + \dfrac{\partial u_1}{\partial x_1} & \lambda_h \dfrac{\partial u_1}{\partial x_2} & 0 \\ \dfrac{\partial u_2}{\partial x_1} & \lambda_h \left(1 + \dfrac{\partial u_2}{\partial x_2}\right) & 0 \\ 0 & 0 & 1 \end{bmatrix} \quad (3.3)$$

$$H_{iJ} = \frac{1}{2} e_{ijk} e_{JKL} \tilde{F}_{jK} \tilde{F}_{kL} \quad (3.4)$$

$$\varepsilon = \frac{\partial u_1}{\partial x_1} + \frac{\partial u_2}{\partial x_2} \quad (3.5)$$

$$\xi_h = \frac{1}{\lambda_h} + \frac{1}{N\nu}\left(\frac{1}{\lambda_h - 1} - \frac{1}{\lambda_h} - \frac{2\chi}{\lambda_h^2}\right) \quad (3.6)$$

In the above equations, $\tilde{F}$ is the deformation gradient tensor relative to the dry state, e_{ijk} is the permutation tensor, and the repeated indices imply summation. The lowercase indices (i, j, k) refer to the coordinates at the swollen state, while the uppercase indices (J, K, L) refer to the dry state. Apparently, the linearized stress–strain relationship for the swollen hydrogel layer, eqn

(3.2), is anisotropic, a result due to the anisotropic deformation of the polymer network during 1-D homogeneous swelling.

For the hydrogel to maintain mechanical equilibrium, the stress field must satisfy the equilibrium equations, namely

$$\frac{\partial s_{11}}{\partial x_1} + \lambda_h \frac{\partial s_{12}}{\partial x_2} = 0 \quad (3.7)$$

$$\frac{\partial s_{21}}{\partial x_1} + \lambda_h \frac{\partial s_{22}}{\partial x_2} = 0 \quad (3.8)$$

In terms of the perturbation displacements, the equilibrium equations become

$$(1 + \lambda_h \xi_h)\frac{\partial^2 u_1}{\partial x_1^2} + \lambda_h^2 \frac{\partial^2 u_1}{\partial x_2^2} + \lambda_h \xi_h \frac{\partial^2 u_2}{\partial x_1 \partial x_2} = 0 \quad (3.9)$$

$$\frac{\partial^2 u_2}{\partial x_1^2} + \lambda_h(\xi_h + \lambda_h)\frac{\partial^2 u_2}{\partial x_2^2} + \lambda_h \xi_h \frac{\partial^2 u_1}{\partial x_1 \partial x_2} = 0 \quad (3.10)$$

In addition, the stress field must satisfy the boundary conditions. Assume a liquid-like surface tension (γ) for the hydrogel. The perturbed surface has a curvature, $\kappa \approx \partial^2 u_2/\partial x_1^2$, to the first-order approximation. By the classical Young–Laplace equation, the normal stress at the surface of the hydrogel layer is balanced by the capillary pressure due to surface tension and the external pressure. In addition, due to the rotation of the surface normal, the nominal traction at the perturbed surface has a shear component. To the first order of purturbation, we have

$$s_{22} = -p\left(1 + \frac{\partial u_1}{\partial x_1}\right) + \gamma \frac{\partial^2 u_2}{\partial x_1^2} \text{ and } s_{12} = p\frac{\partial u_2}{\partial x_1} \text{ at } x_2 = h \quad (3.11)$$

where $h = \lambda_h h_0$ is the thickness of the hydrogel layer at the swollen state. At the hydrogel/substrate interface, we assume perfect bonding with zero displacements, i.e., $u_1 = u_2 = 0$ at $x_2 = 0$.

By the method of Fourier transform we solve the equilibrium equations (3.9)-(3.10) and obtain that

$$\hat{u}_1(x_2; k) = \sum_{n=1}^{4} A_n \bar{u}_1^{(n)} \exp(q_n x_2) \quad (3.12)$$

$$\hat{u}_2(x_2; k) = \sum_{n=1}^{4} A_n \bar{u}_2^{(n)} \exp(q_n x_2) \quad (3.13)$$

where $\hat{u}_1(x_2; k)$ and $\hat{u}_2(x_2; k)$ are the Fourier transforms of the displacements, $u_1(x_1, x_2)$ and $u_2(x_1, x_2)$, with respect to x_1, and k is the Fourier wave number. The four eigenvalues are obtained from the equilibrium equations as

$$q_{1,2} = \pm \frac{k}{\lambda_h} \text{ and } q_{3,4} = \pm \beta k \quad (3.14)$$

where $\beta = \sqrt{(1 + \lambda_h \xi_h)/(\lambda_h^2 + \lambda_h \xi_h)}$. Correspondingly, we have the eigenvectors,

$$\begin{bmatrix} \bar{u}_1^{(1)} & \bar{u}_1^{(2)} & \bar{u}_1^{(3)} & \bar{u}_1^{(4)} \\ \bar{u}_2^{(1)} & \bar{u}_2^{(2)} & \bar{u}_2^{(3)} & \bar{u}_2^{(4)} \end{bmatrix} = \begin{bmatrix} 1 & 1 & 1 & 1 \\ -i\lambda_h & i\lambda_h & -i\beta & i\beta \end{bmatrix} \quad (3.15)$$

We note that, for each Fourier component with a specific wave number k, the perturbation displacement is periodic in the x_1

direction, but varies exponentially in the x_2 direction for each eigen mode, similar to Biot's analysis for surface instability of a half-space rubber-like material under mechanical compression.[10]

Next applying the boundary conditions, we obtain that

$$\sum_{n=1}^{4} D_{mn}A_n = 0 \qquad (3.16)$$

where the coefficient matrix is given by

$$D = \begin{bmatrix} 1 & 1 \\ -\lambda_h & \lambda_h \\ (2+kL)\lambda_h e^{kh_0} & (2-kL)\lambda_h e^{-kh_0} \\ \left(\lambda_h + \frac{1}{\lambda_h}\right)e^{kh_0} & -\left(\lambda_h + \frac{1}{\lambda_h}\right)e^{-kh_0} \\ 1 & 1 \\ -\beta & \beta \\ \left(\lambda_h + \frac{1}{\lambda_h} + \beta kL\right)e^{\beta kh} & \left(\lambda_h + \frac{1}{\lambda_h} - \beta kL\right)e^{-\beta kh} \\ 2\beta e^{\beta kh} & -2\beta e^{-\beta kh} \end{bmatrix} \qquad (3.17)$$

with $L = \gamma/(Nk_BT)$. The critical condition for swell-induced surface instability of the hydrogel layer is then obtained by setting the determinant of the matrix $\mathbf{D}$ to be zero, namely

$$\text{Det}[\mathbf{D}] = f\left(kh_0, \lambda_h, \frac{h_0}{L}, Nv, \chi\right) = 0 \qquad (3.18)$$

We postpone the discussions on the results of the linear perturbation analysis till next section. Here we note that the ratio between the surface tension (γ) and the bulk shear modulus ($G_0 = Nk_BT$) of the polymer network defines an intrinsic length scale (L). A similar length scale appeared in a critical condition that predicts the maximum pressure for cavitation in hydrogels.[25] Alternatively, a length scale can be defined with respect to the molecular volume of solvent, *i.e.*, $L' = \gamma v/(k_BT)$, which is independent of the polymer network. Take the surface tension of the hydrogel to be similar to that of water.[25] At the room temperature, $\gamma \sim 0.073$ N/m and $v \sim 3 \times 10^{-29}$ m³, we have $L' \sim 0.53$ nm, while the length L can vary over several orders of magnitude (from nanometers to micrometers) depending on the value of Nv. It turns out that the same length scale (L) could result in a size-dependent swelling ratio for nanoscale hydrogel particles.[24] In the present study, we show that the presence of such a length scale leads to a thickness-dependent critical condition for swell-induced surface instability of substrate-confined hydrogel layers.

4. Results and discussions

The linear perturbation analysis predicts a critical condition, eqn (3.18), for onset of swell-induced surface instability of substrate-confined hydrogel layers. As plotted in Fig. 2a, the predicted critical swelling ratio (λ_c) is a function of the normalized perturbation wavelength, $S = 2\pi/(kh_0)$, depending on the initial layer thickness (h_0) as well as the material properties (Nv, χ, and $\bar{p}_0$) of the hydrogel. Fig. 2b plots the corresponding critical
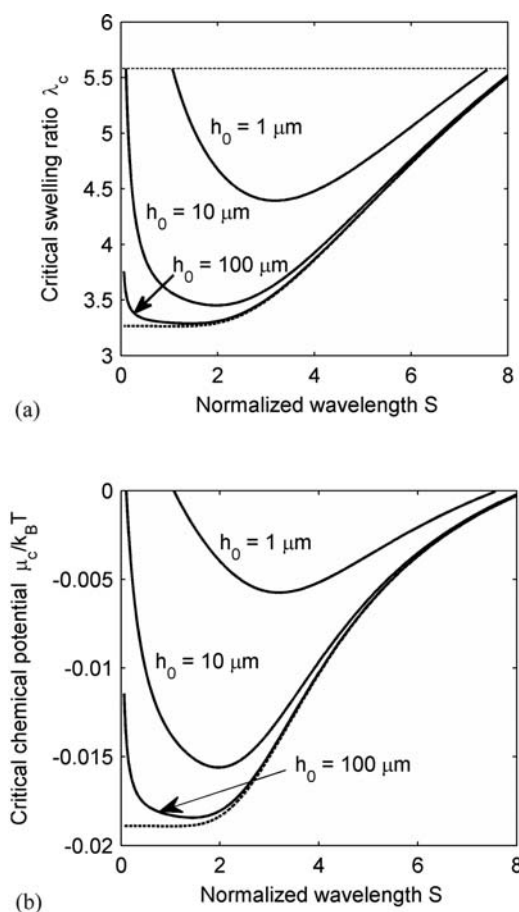

(a)

(b)

Fig. 2 (a) Critical swelling ratio and (b) critical chemical potential, versus the perturbation wavelength for swell-induced surface instability of substrate-confined hydrogel layers with $Nv = 10^{-3}$, $\chi = 0.4$, and $L = 0.53$ μm. The thick dashed lines show the results without the effect of surface tension, and the thin dashed line in (a) indicates the homogeneous swelling ratio at equilibrium.

chemical potential (μ_c), which is related to the critical swelling ratio by eqn (2.1). For these calculations, we assume a specific hydrogel system with $Nv = 10^{-3}$, $\chi = 0.4$, $\bar{p}_0 = 2.3 \times 10^{-5}$, and $L = 0.53$ μm. For comparison, the thick dashed lines in Fig. 2 show the results from the previous analysis with no surface effect, which are independent of the layer thickness. As expected, the surface tension tends to stabilize short-wavelength perturbations, leading to increasingly larger critical swelling ratio as the wavelength decreases. Together with the effect of substrate confinement, which suppresses the long-wavelength perturbations, the critical swelling ratio has a minimum (λ_c^*) at an intermediate wavelength (S^*); both λ_c^* and S^* depend on the initial thickness (h_0) of the hydrogel layer.

Fig. 3a plots the minimum critical swelling ratio (λ_c^*) as a function of the initial thickness (h_0) of the hydrogel layer, and Fig. 3b plots the corresponding wavelength (S^*h_0). To illustrate the effect of surface tension, the results are shown for different values of the length scale L. As a dimensionless quantity, the minimum critical swelling ratio depends on the ratio between the two lengths, h_0/L. For a relatively thick hydrogel layer, the surface tension has negligible effect, and thus the critical swelling ratio approaches the previous prediction (the lower dashed line),
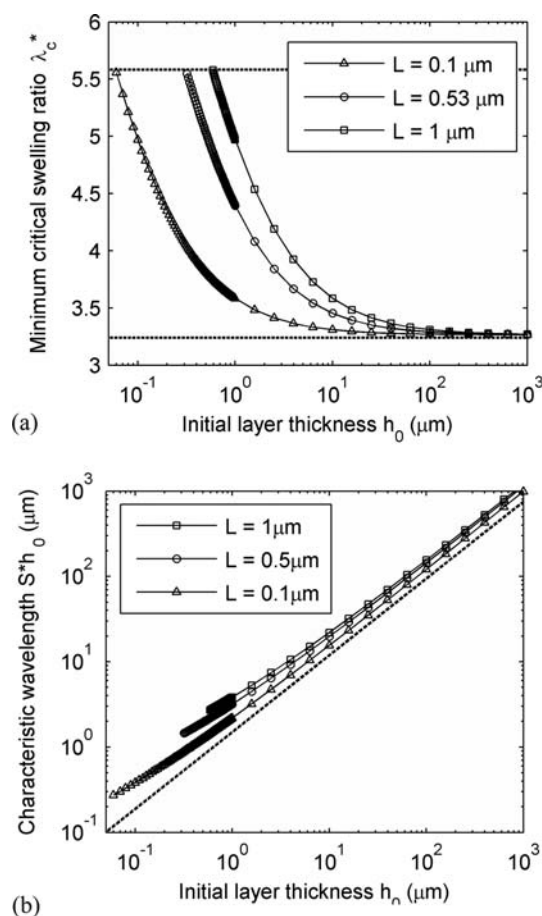
Fig. 3 (a) The minimum critical swelling ratio and (b) the corresponding characteristic wavelength, versus the initial thickness of the substrate-confined hydrogel layers with $Nv = 10^{-3}$ and $\chi = 0.4$. The lower dashed line in (a) shows the thickness-independent critical swelling ratio without the effect of surface tension, and the upper dashed line indicates the homogeneous swelling ratio at equilibrium. The dashed line in (b) shows the power-law scaling of the characteristic wavelength, $S^*h_0 \sim h_0^{0.9}$.

which is independent of the layer thickness. As the layer thickness decreases, the effect of surface tension becomes increasingly important, and the critical swelling ratio increases until it reaches the equilibrium homogeneous swelling ratio (the upper dashed line) of the hydrogel layer at a critical thickness (h_c). For a thinner hydrogel layer ($h_0 < h_c$), the homogeneous swelling is stable up to the equilibrium chemical potential ($\hat{\mu} = 0$). Corresponding to the minimum critical swelling ratio, the characteristic wavelength (S^*h_0) decreases monotonically as the layer thickness decreases (Fig. 3b), in qualitative agreement with experimental observations.[4,6–8] However, it is found that the characteristic wavelength as predicted here is not exactly proportional to the layer thickness. Instead, it appears to approximately follow a power-law scaling,

$$S^*h_0 \propto h_0^{1-\alpha} L^\alpha \qquad (4.1)$$

with a positive exponent α, over a wide range of the layer thickness. As shown by the dashed line in Fig. 3b, $\alpha \approx 0.1$ for $Nv = 10^{-3}$ and $\chi = 0.4$. The positive exponent (α) suggests that the characteristic wavelength increases as the surface tension of

the hydrogel increases. Remarkably, the exponent is found to be insensitive to the other material properties of the hydrogel, with nearly identical value of α for different Nv and χ.

It is of interest to note that, while the surface tension has no effect on homogeneous swelling of a substrate-confined hydrogel layer, it plays a critical role in stabilizing thin hydrogel layers. In particular, the critical thickness (h_c) for a stable hydrogel layer is linearly proportional to the length scale L, which in turn is proportional to the surface tension γ. Similar critical thickness exists for surface instability of epitaxial crystal thin films.[26] Fig. 4 plots the critical thickness (h_c) as a function of Nv for different values of χ, assuming a constant value for L'. The critical thickness depends on Nv through two competing factors. First, for a constant surface tension (γ) and solvent molecular volume (v), because the length scale L decreases with increasing Nv, the critical thickness tends to decrease as well. On the other hand, since the polymer network of the hydrogel becomes increasingly stiff as Nv increases, the degree of swelling decreases. With less swelling, the hydrogel layer is more stable, and the critical thickness tends to increase. Consequently, the ratio between the critical thickness and the length scale, h_c/L, increases monotonically with increasing Nv. When Nv is relatively small, the effect of surface tension dominates, and the critical thickness decreases with increasing Nv. The trend is reversed as the elasticity of polymer network becomes significant with relatively large Nv. On the other hand, the dependence of the critical thickness on χ is simpler. As χ increases, the degree of swelling decreases and the critical thickness increases. For χ greater than a critical value ($\chi_c \sim 0.63$), the hydrogel layer remains stable at the equilibrium swelling state.[15] For each χ less than the critical value, there exists a maximum value for Nv, beyond which the critical thickness is essentially infinity. This again is attributed to limited degree of swelling, with which the hydrogel layer of any thickness would remain stable at the equilibrium state. Therefore, the critical condition for swell-induced surface instability of the substrate-confined hydrogel layer is largely determined by the three dimensionless parameters: h_0/L, Nv, and χ. As shown in Fig. 4, for typical values of Nv and χ, the critical thickness ranges between 100 nm and 1 μm. As shown in Fig. 3a, the critical thickness decreases as the length scale (L) decreases. When the
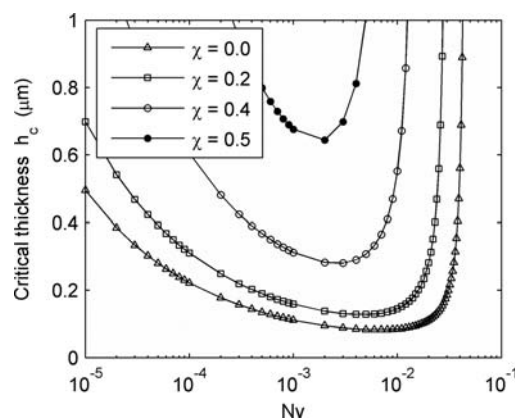

Fig. 4 The critical thickness of substrate-confined hydrogel layers, predicted as a function of Nv for various values of χ. The length scale L' is assumed to be a constant ($L' = 0.53$ nm).

hydrogel is immersed in water, the surface tension of the gel/water interface may be smaller than that of the water/air interface,[27] which then leads to a smaller length scale (L) and thus smaller critical thickness.

As noted in the previous study,[15] the present stability analysis assumes a quasi-statically controlled swelling process, where the hydrogel layer swells homogeneously until the onset of surface instability. As such, the effect of swelling kinetics has been ignored. In experiments, when a hydrogel layer is immersed in a solvent, the transient state of swelling is typically inhomogeneous and the stability condition depends on the kinetics.[4,17] Three scenarios may occur. First, the hydrogel layer remains stable and swells homogeneously up to the equilibrium state. This was observed for gels when the degree of swelling is relatively small.[4] Second, the hydrogel layer becomes unstable and develops surface creases during the transient swelling process. Eventually as the hydrogel layer reaches the equilibrium state, the surface creases disappear, and the equilibrium state of homogeneous swelling is stable.[4] Third, the surface creases develop and evolve during the transient process, and remain at the equilibrium state,[6] suggesting that the homogeneous swelling is unstable at the equilibrium state. The critical condition for surface instability as developed in the present study predicts whether the equilibrium state of homogeneous swelling is stable, but does not predict the onset of surface instability during the transient process. It is speculated that the critical swelling ratio for surface instability could be considerably lower for inhomogeneous swelling at the transient state. The detailed analysis on the effect of swelling kinetics is left for a separate study.

Another interesting point to note is the effect of temperature on swell-induced surface instability of hydrogels. Within the present model, we see several possible effects that depend on temperature. First, in eqn (2.1), the homogeneous swelling ratio depends on temperature through the normalized vapor pressure, $\bar{p}_0 = p_0 v/(k_B T)$, where p_0 itself is a function of temperature. In addition, the other material properties (N, χ, and v) may all depend on temperature. Experimentally it has been observed that polymer gels may undergo continuous or discontinuous volume phase transition as the temperature changes,[28] suggesting possible changes in the structure of the polymer network as well as the interaction between the polymer and the solvent molecules. In the stability analysis, as the surface tension may depend on temperature, the predicted critical swelling ratio, the characteristic wavelength, and the critical layer thickness all depend on temperature. It is thus possible that a hydrogel layer is stable at one temperature but becomes unstable at a different temperature. In addition, it is well known that the kinetics of mass transport and swelling is typically sensitive to temperature. Therefore, the effect of temperature on swell-induced surface instability of hydrogels is in general complicated with convolution of multiple effects on the material parameters and physical processes.

5. Concluding remarks

This paper presents a theoretical analysis on swell-induced surface instability of substrate-confined hydrogel layers. In particular, the effect of surface tension is highlighted in comparison with a previous study[15] that considered the effect of substrate confinement alone. With both surface tension and substrate confinement, we show that the stability of a hydrogel layer depends on its initial thickness. A critical thickness is thus predicted, which is proportional to the surface tension and depends on the other material parameters of the hydrogel. The onset of surface instability is predicted at a characteristic wavelength with the minimum critical swelling ratio. An approximate power-law scaling for the characteristic wavelength is suggested. The minimum critical swelling ratio decreases as the layer thickness increases, depending on the ratio between the two length scales (h_0/L) and approaching a constant at relatively large thickness.

Finally we note that the linear perturbation analysis in the present study assumes a smooth surface perturbation onto a homogeneously swollen hydrogel layer at the onset of surface instability. This is in the same spirit as Biot's analysis on surface instability of a half-space rubber under mechanical compression,[10] but different from the energetic analysis by Hong et al.[11] As shown by numerical simulations in our previous study,[15] the smooth surface perturbation can subsequently evolve to form localized features such as grooves and creases (Fig. 1c), as a result of nonlinear post-instability evolution. More studies, both theoretical and experimental, are needed to further elucidate the nonlinear process of swell-induced surface evolution as well as the relationship between the two types of surface instability patterns.

Acknowledgements

Notes and references

1 A. N. Gent and I. S. Cho, *Rubber Chemistry and Technology*, 1999, **72**, 253–262.
2 A. Ghatak and A. L. Das, *Phys. Rev. Lett.*, 2007, **99**, 076101.
3 E. Southern and A. G. Thomas, *J. Polymer Science A*, 1965, **3**, 641–646.
4 T. Tanaka, S.-T. Sun, Y. Hirokawa, S. Katayama, J. Kucera, Y. Hirose and T. Amiya, *Nature*, 1987, **325**, 796–798.
5 H. Tanaka, H. Tomita, A. Takasu, T. Hayashi and T. Nishi, *Phys. Rev. Lett.*, 1992, **68**, 2794–2797.
6 V. Trujillo, J. Kim and R. C. Hayward, *Soft Matter*, 2008, **4**, 564–569.
7 M. Guvendiren, S. Yang and J. A. Burdick, *Adv. Funct. Mater.*, 2009, **19**, 3038–3045.
8 E. P. Chan, E. J. Smith, R. C. Hayward and A. J. Crosby, *Adv. Mater.*, 2008, **20**, 711–716.
9 J. Kim, J. Yoon and R. C. Hayward, *Nat. Mater.*, 2010, **9**, 159–164.
10 M. A. Biot, *Appl. Sci. Res. A*, 1963, **12**, 168–182.
11 W. Hong, X. Zhao and Z. Suo, *Appl. Phys. Lett.*, 2009, **95**, 111901.
12 K. Sekimoto and K. Kawasaki, *J. Phys. Soc. Jpn.*, 1987, **56**, 2997–3000.
13 A. Onuki, *Phys. Rev. A: At., Mol., Opt. Phys.*, 1989, **39**, 5932–5948.
14 N. Suematsu, K. Sekimoto and K. Kawasaki, *Phys. Rev. A: At., Mol., Opt. Phys.*, 1990, **41**, 5751–5754.
15 M. K. Kang and R. Huang, *J. Mech. Phys. Solids*, DOI: 10.1016/j.jmps.2010.07.008, Preprint available online at http://www.imechanica.org/node/7587.
16 T. Tomari and M. Doi, *J. Phys. Soc. Jpn.*, 1994, **63**, 2093–2101.
17 M. Doi, *J. Phys. Soc. Jpn.*, 2009, **78**, 052001.
18 R. Huang and Z. Suo, *J. Appl. Phys.*, 2002, **91**, 1135–1142.
19 R. Huang, *J. Mech. Phys. Solids*, 2005, **53**, 63–89.
20 R. Huang and S. H. Im, *Phys. Rev. E: Stat., Nonlinear, Soft Matter Phys.*, 2006, **74**, 026214.

21 P. J. Flory, *Principles of Polymer Chemistry*, Cornell University Press, Ithaca, NY, 1953.

22 W. Hong, X. Zhao, J. Zhou and Z. Suo, *J. Mech. Phys. Solids*, 2008, **56**, 1779–1793.

23 M. K. Kang and R. Huang, *J. Appl. Mech.*, 2010, DOI: 10.1115/1.4001715, Preprint available online at http://www.imechanica.org/node/6594.

24 R. Huang, unpublished work.

25 S. Kundu and A. J. Crosby, *Soft Matter*, 2009, **5**, 3963–3968.

26 Y. Pang and R. Huang, *Phys. Rev. B: Condens. Matter Mater. Phys.*, 2006, **74**, 075413.

27 J. F. Joanny, A. Johner and T. A. Vilgis, *Eur. Phys. J. E*, 2001, **6**, 201–209.

28 Y. Li and T. Tanaka, *Annu. Rev. Mater. Sci.*, 1992, **22**, 243–277.